Published in final edited form as:
Neurotoxicology. 2012 October ; 33(5): 996–1004. doi:10.1016/j.neuro.2012.04.014.

Intranasal exposure to manganese disrupts neurotransmitter release from glutamatergic synapses in the central nervous system *in vivo*

Andrew H. Moberly[*], **Lindsey A. Czarnecki**[*], **Joseph Pottackal**, **Tom Rubinstein**, **Daniel J. Turkel**, **Marley D. Kass**, and **John P. McGann**
Behavioral Neuroscience Section, Department of Psychology, Rutgers, The State University of New Jersey

Abstract

Chronic exposure to aerosolized manganese induces a neurological disorder that includes extrapyramidal motor symptoms and cognitive impairment. Inhaled manganese can bypass the blood-brain barrier and reach the central nervous system by transport down the olfactory nerve to the brain's olfactory bulb. However, the mechanism by which Mn disrupts neural function remains unclear. Here we used optical imaging techniques to visualize exocytosis in olfactory nerve terminals *in vivo* in the mouse olfactory bulb. Acute Mn exposure via intranasal instillation of 2–200 μg $MnCl_2$ solution caused a dose-dependent reduction in odorant-evoked neurotransmitter release, with significant effects at as little as 2 μg $MnCl_2$ and a 90% reduction compared to vehicle controls with a 200 μg exposure. This reduction was also observed in response to direct electrical stimulation of the olfactory nerve layer in the olfactory bulb, demonstrating that Mn's action is occurring centrally, not peripherally. This is the first direct evidence that Mn intoxication can disrupt neurotransmitter release, and is consistent with previous work suggesting that chronic Mn exposure limits amphetamine-induced dopamine increases in the basal ganglia despite normal levels of dopamine synthesis (Guilarte et al., *J Neurochem* 2008). The commonality of Mn's action between glutamatergic neurons in the olfactory bulb and dopaminergic neurons in the basal ganglia suggests that a disruption of neurotransmitter release may be a general consequence wherever Mn accumulates in the brain and could underlie its pleiotropic effects.

Keywords

Manganese; Olfactory; Olfaction; Imaging; Pathophysiology; Exocytosis

1. Introduction

Manganese is a heavy metal that is an essential nutrient at very low concentrations and a neurotoxicant at high concentrations (Aschner et al., 2009; Mergler et al., 1999).

Corresponding author, John P. McGann, PhD, Department of Psychology, Rutgers University, 152 Frelinghuysen Road, Piscataway, NJ 08854 USA, jmcgann@rci.rutgers.edu, Phone: 617-519-7232.
[*]These authors contributed equally to this report.

The authors declare no conflicts of interest.

Environmental exposure to high concentrations of manganese (typically aerosolized in certain industrial workplaces) causes a movement disorder characterized by extrapyramidal motor dysfunctions including bradykinesia, akinetic rigidity, and dystonia (Couper 1837; Cerosimo and Koller 2006; Pal et al., 1999; Barbeau et al., 1976). This disorder, known as manganism, is distinct from idiopathic Parkinson's disease (Guilarte, 2010a; Perland Olanow 2007), though Mn exposure makes the development of idiopathic Parkinson's disease more likely and more rapid (Racette et al., 2005; Willis et al., 2010). Lower doses or briefer exposures to Mn have been associated with psychotic symptoms, impairment in short term memory, attention, and fine motor control, olfactory deficits, as well as worsened mood (Iregren 1994; Bowler et al., 1999; Roels et al., 1985; Roels et al., 1992; Laohaudomchok et al., 2011; Antunes et al., 2007), effects which may persist even long after exposure ceases (Bouchard et al., 2007). Consistent with this broad spectrum of symptoms, exposure to manganese in animal models can induce neurotoxicity in multiple brain regions, including the basal ganglia (Pentschew et al., 1963; Eriksson et al., 1987; reviewed in Guilarte 2010a), frontal cortex (Guilarte et al., 2008a; Guilarte 2010b; Dydak et al., 2011), and olfactory pathways (Henriksson and Tjälve 2000), typically after multiple exposures.

Manganese distributes non-uniformly in the brain, with particular concentrations naturally occurring in the basal ganglia and olfactory bulbs of naïve (non-exposed) rats (Donaldson et al., 1974), non-exposed humans at autopsy (Bonilla et al., 1982), and rodents and non-human primates exposed chronically via repeated ip injections (Bonilla et al., 1994; Guilarte et al., 2008b). The reason for this distinctive accumulation pattern in these two brain regions is uncertain, but may result from regional differences in the expression of metal-binding peptides like metallothioneins or carnosine (Sunderman et al., 2001). The most common route of exposure to high concentrations of manganese is intranasal, through the inhalation of Mn fumes and dusts, which also leads to increased Mn concentrations in the olfactory bulbs and basal ganglia (Vitarella et al., 2000; Brenneman et al., 2000; Dorman et al., 2002). With acute intranasal exposures (50–800 μg $MnCl_2$), Mn is taken up by the olfactory epithelium in the upper airway, including both sustentacular cells, from which it can reach the bloodstream (Gianutsos et al., 1997; Thompson et al., 2007; Thompson et al., 2011) and olfactory receptor neurons (ORNs), from which it can be transported into the central nervous system (Thompson et al., 2011; Tjälve et al., 1996). It has recently been shown that intact ORN axonal projections from the olfactory epithelium to the olfactory bulb are necessary for Mn transport from the nasal cavity to the brain (Thompson et al., 2011).

The mechanisms of Mn-induced neurotoxicity are complex and incompletely understood. Expression of manganese superoxide dismutase, an essential antioxidant found in mitochondria, is upregulated in the brain following repeated ip injections of 2.5 or 5 mg $MnCl_2$/kg (Hussain et al., 1997), and higher doses of Mn may induce oxidative damage (Desole et al., 1995; Taylor et al., 2006; Milatovic et al., 2011; but see Brenneman et al., 1999). Mn-induced impairment in mitochondrial function can disrupt neuronal energy supplies, which may make the neurons vulnerable to excitotoxicity and degeneration (Wedler et al., 1989; Brouillet et al., 1993; Gavin et al., 1999). Mn-exposure also stimulates a range of neuroinflammatory signaling cascades via action on glial cells in culture (Spranger et al., 1998; Zhang et al., 2009; Barhoumi et al., 2004)as well as in mice orally exposed to 100 mg $MnCl_2$/kg once daily for eight weeks (Liu et al., 2006).. However, these mechanisms do not directly address the physiological changes that must underlie the complex neurobehavioral deficits observed following manganese exposure.

Limited evidence suggests that Mn exposure disrupts neurotransmitter signaling in the brain. In astrocyte cultures exposure to 100–500 μM $MnCl_2$ for 24–48 hours reduces the uptake of aspartate and glutamate (Hazell and Norenberg 1997; Erikson and Aschner 2002), the principal excitatory neurotransmitter in the brain (Cotman et al., 1981). This is likely due to

a downregulation of the glutamate-aspartate transporter (Erikson and Aschner 2002). Notably, recent molecular imaging in the basal ganglia of Mn-exposed primates (weekly iv injections of 10–30 mg $MnSO_4$/kg) has shown significant reductions in amphetamine-evoked dopamine release (Guilarte et al., 2006; Guilarte et al., 2008b) despite normal baseline dopamine levels, suggesting that one action of manganese might be a disruption of presynaptic function (see Discussion). Similarly, perfusion of the hippocampus with 60 μL of an artificial cerebrospinal fluid containing 200 nM $MnCl_2$reduced the concentrations of glutamate and GABA in the perfusate, while a 20 nM concentration reduced only glutamate concentration (Takeda et al., 2002).

We have recently demonstrated the utility and sensitivity of optical imaging from the mouse olfactory system to visualize toxicant-induced changes in neurotransmitter release from ORN presynaptic terminals *in vivo* (Czarnecki et al., 2011). This is accomplished in a line of transgenic mice expressing the synaptopHluorin (spH) construct (Miesenböck et al., 1998) in all ORN axon terminals from the locus for olfactory marker protein (OMP) (Bozza et al., 2004). In these OMP-spH mice the rapid increase in intravesicular pH during exocytosis causes a rapid and proportional increase in green fluorescent protein (GFP) fluorescence that linearly indicates transmitter release from the olfactory nerve into olfactory bulb glomeruli (Wachowiak et al., 2005). Odorants reaching the olfactory epithelium bind to a subset of olfactory receptors and thus drive synaptic input to a corresponding subset of olfactory bulb glomeruli (Mombaerts et al., 1996), which exhibit dramatic, odorant-specific increases in fluorescence in these mice (Bozza et al., 2004). Patterns of odorant-evoked synaptic input from the olfactory nerve to the olfactory bulb are typically bilateral and approximately symmetric (Bozza et al., 2004; Soucy et al., 2009) including after bilateral intranasal vehicle infusions of the sort performed here (Czarnecki et al., 2011). Because the nasal passages are separated by a medial septum and the olfactory nerves project exclusively ipsilaterally to the olfactory bulb, it is possible to selectively expose one side to a neurotoxicant and compare the observed responses to the contralateral control side (Czarnecki et al., 2011). Here we test the hypothesis that one intranasal exposure to 2–200 μg of $MnCl_2$ reduces stimulus-evoked neurotransmitter release in a dose-dependent manner.

2. Material and Methods

2.1 Subjects

Subjects in the imaging experiments were 24 homozygous male and female OMP-spH mice, which express the spH construct (Miesenböck et al., 1998) from the locus for OMP (Bozza et al., 2004). Four additional OMP-spH mice were used for olfactory bulb histology. The mice used in this study are on an albino C57Bl/6 background as previously reported (Czarnecki et al., 2011). All animals were group housed with a 12:12 h light:dark cycle with food and water available *ad libitum.* All procedures were performed in accordance with protocols approved by the Rutgers University Animal Care and Use Committee.

2.2 Intranasal infusions

Mice in Mn-exposed groups received intranasal instillations (see Czarnecki et al., 2011) of 6 μL of pH 7.4 buffer solution containing 200 mM HEPES, 0.9% NaCl, and either 265 mM, 26.5 mM, or 2.65 mM $MnCl_2$ as noted. These concentrations yield individual infusions of 200 μg, 20 μg, and 2 μg of manganese chloride, respectively. For imaging experiments, each mouse received an infusion of manganese solution into one external naris and vehicle solution (without $MnCl_2$) into the contralateral naris, with side counterbalanced across subjects. Because the nasal passages on the left and right sides are separated by a nasal septum and the ORN projections are strictly ipsilateral, this design permitted within-subjects, left vs. right comparisons. Animals were lightly anesthetized with 1000μg/kg

metatomadine and 70mg/kg ketamine administered by intraperitoneal (i.p.) injection. An Eppendorf microloader attached to a 10μL Hamilton syringe containing the infusate was inserted 7 mm into one naris in order for the solution to reach the olfactory epithelium. The mouse was placed on its back, and the infusion was delivered. The animal remained on its back for five minutes and was then rotated to its side for another 20 minutes to ensure coverage across the epithelium. The procedure was repeated for the other naris. Anesthesia was then reversed by subcutaneous (s.c.) injection of 1mg/kg atipamezole hydrochloride. Reflux of solution was not observed. The experimenter was blind to the contents of all infusates. Animals were imaged two days following intranasal instillation, the earliest time point that allowed for recovery from any potential mechanical effects of the physical insertion of the microloader into the naris and to allow full recovery from the anesthetic.

2.3 In vivo imaging of neurotransmitter release

Two days after unilateral intranasal manganese exposure, mice underwent optical imaging as previously reported (Czarnecki et al., 2011). Briefly, mice were anesthetized with 0.01 mL/g pentobarbital (i.p.) with 0.05 mL boosters as needed to maintain anesthetic plane. Body temperature was maintained using a feedback-regulated heating pad and a rectal thermistor probe. Mice were administered 0.005 mL of 0.1% atropine sulfate (s.c.) to reduce nasal secretions and about 0.25 mL 0.1% bupivicaine hydrochloride (s.c.) as a local anesthetic under the scalp. The scalp was surgically opened with a midline incision, the periosteal membrane was removed, and the skull was dried with a 70% ethanol solution. A headbar was fixed to the skull using dental acrylic to rigidly mount the mouse's skull to a custom headholder. Using a micromotor dental handpiece, the skull overlying both olfactory bulbs was thinned until transparent when wet. Ringer's solution (140 mM NaCl, 5 mM KCl, 1 mM $CaCl_2$, 10 mM HEPES, and 10 mM dextrose, pH 7.4) was applied over this cranial window and then topped with a glass coverslip.

Optical imaging was performed using a custom apparatus for fluorescence imaging as previously described (Czarnecki et al., 2011). Epiillumination was provided by an Opti-Quip 150W Xenon arc lamp with appropriate neutral density filters. For bilateral imaging of odorant-evoked responses we used an Olympus XLFluor4X macro objective (0.28 NA), while we used an Olympus XLUMPlanFl 10X water immersion objective (0.60 NA) during focal nerve stimulation. Images were acquired using a RedShirtImaging monochrome, back-illuminated CCD camera (NeuroCCD SM256) at 256 x 256 pixel resolution and frame acquisition rate of 7 Hz (odorant stimulation) or 25 Hz (electrical stimulation). The mouse was positioned under the microscope using a custom 3-axis optomechanical stage. The entire apparatus floated on a vibration isolation table.

Odorants were presented by a custom built eight-channel, air dilution olfactometer controlled by a computer running software written for MatLab (Mathworks). Purified nitrogen was the carrier vapor, which was saturated in the headspace of an odorant vial and then diluted into purified ultra-zero humidity air in a ratio determined by a pair of mass flow controllers. Odorants were presented to the animal's nose using a pair of concentric glass tubes, of which the inner tube delivered the odorant and the outer, slightly longer tube carried a vacuum that normally removed the odorant before it reached the animal. Odorant onset and offset were controlled by a computer-operated valve that shunted the vacuum away from the odorant removal tube during odorant presentation and then back to the odorant removal tube afterwards. Monomolecular odorants included methyl valerate, 2-methyl-2-butenal, 2-hexanone and butyl acetate, which are known to evoke transmitter release on the dorsal aspect of the olfactory bulb (Wachowiak and Cohen, 2001; Bozza et al., 2004; Soucy et al., 2009). Odorants were presented in 6 s trials at a 0.5–4% dilution of saturated vapor. The minimum intertrial interval was 60 s. The experimenter was blind to

the experimental condition of the mouse. Odorant concentrations were standardized across sessions using a photoionization detector (ppbRae, Rae Systems).

2.4 In vivo nerve stimulation

For *in vivo* nerve stimulation (Pírez and Wachowiak, 2008), the bone overlying the olfactory bulbs was removed and the dura overlying the dorsal olfactory bulbs carefully cut and peeled away. Using a motorized micromanipulator (Sutter MP-225), a concentric bipolar electrode with a 25 μm tip was positioned onto an afferent bundle of ORN axons under fluorescence visual guidance. Electrical stimuli were single 100 μs constant current pulses at 6–60 μA.

2.5 Imaging data analysis

Imaging data were analyzed as described previously (Czarnecki et al., 2011). Briefly, blank trials on which no stimuli were presented were subtracted from each stimulus-present trial to correct for photobleaching, a ubiquitous, stimulus-independent reduction in fluorescence caused by excitation of the fluorophore. Stimulus-evoked glomerular responses were measured as the average of 15 frames centered on the peak of the fluorescence increase minus the average of 15 baseline frames immediately prior to stimulus onset. Trials were treated individually for amplitude measurements and averaged within odorants to create spatial maps of odorant-evoked responses. Candidate regions of interest corresponding to olfactory bulb glomeruli were initially selected by hand in Neuroplex (RedShirtImaging) and then confirmed statistically. Changes in fluorescence for each region of interest on each trial were extracted using custom software written in MatLab. A glomerulus was operationally defined as responding to an odorant if its average increase in fluorescence across trials of that odorant was greater than zero by three standard errors or more. The number of statistically-confirmed glomerular responses in the olfactory bulb ipsilateral to the cadmium-exposed naris was divided by the number of glomerular responses in the olfactory bulb ipsilateral to the vehicle-exposed naris to compute a within-subjects ratio of the number of observed responses. A ratio of 1 would indicate that there were an equal number of glomeruli responding to odorants on both Mn-exposed and vehicle-exposed sides, while a ratio less than one would indicate that fewer glomeruli responded to odorants on the Mn-exposed side than on the vehicle-exposed side. Analyzed data were compiled and organized in Excel, plotted in SigmaPlot, and analyzed statically using SPSS (see below).

2.6 Olfactory bulb histology and immunohistochemistry

As previously reported (Czarnecki et al., 2011), after imaging mice were intracardially perfused with 0.1M phosphate-buffered solution (PBS) followed by 4% paraformaldehyde/PBS solution for perfusion and postfixation. Brains were blocked to include both olfactory bulbs and the frontal cortex and sectioned horizontally at 50 μm on a vibratome. For immunohistochemistry, free floating sections were blocked for 3 minutes at room temperature in 10% normal goat serum (NGS), 1% bovine serum albumin (BSA) and 0.3% Triton X-100 in 0.1M PBS. Sections were then incubated overnight at 4°C in carrier solution (1% NGS, 1% BSA, 0.3% Triton in PBS) containing primary antibody against tyrosine hydroxylase (rabbit anti-mouse TH, 1:1000 dilution, Millipore #AB152) or calbindin-d28k (rabbit anti-mouse CBD, 1:500 dilution, Millipore #AB1778) in alternate sections. Primary antibody was excluded from one section in each reaction as a control; these sections never exhibited immunofluorescence. Sections were rinsed three times in carrier solution, then incubated for two hours at room temperature in 10 μg/mL fluorophore-tagged secondary antibody (goat anti-rabbit IgG H+L conjugated to AlexaFluor568, Invitrogen #A-11011). One section from each reaction excluded secondary antibody as a control. Sections were mounted in ProLong Gold antifade reagent (Invitrogen) containing the nuclear counterstain 4′,6-diamidino-2-phenylindole (DAPI) on glass slides and sealed under a glass coverslip.

Photos of olfactory bulb sections were taken at a resolution of 1360 × 1024 pixels and 14 bit analog-to-digital conversion with a Jenoptik MFcool Peltier-cooled monochrome CCD camera mounted on an Olympus BX41 microscope at 4X (0.16 NA). Images were opened in ImageJ (NIH) and the glomerular layer of each olfactory bulb was selected as a region of interest based on the rings of periglomerular interneurons visualized by the DAPI stain (thus providing an unbiased means of selecting regions of interest). The optical density of these regions of interest was then measured in the corresponding image taken using appropriate optical filters for each fluorophore (the Green Fluorescent Protein-based synaptopHluorin as a marker of ORN afferents or the AlexaFluor568 as a marker for the secondary antibody). Experimenters were blind to the experimental condition of the animal until after the quantification was completed.

2.7 Statistical analyses

Descriptive statistics are reported mean (± standard error). Analysis of variance was performed to test statistically for differences between the means of experimental groups following random assignment of subjects, as described above. To test for statistical difference from a hypothesized value, a one-sample t-test was used. To compare distributions of glomerular response amplitudes (which may differ along dimensions other than central tendency) between groups we use the nonparametric Kolmogorov-Smirnov (K-S) and Mann-Whitney U-tests to test the model that both distributions are samples from the same underlying distribution. To compare differences in the count of electrically-evoked responses between treatment groups, a Chi Square (χ^2) test appropriate for categorical data was used. All statistical testing was performed using SPSS.

3. Results

3.1 Intranasal manganese exposure disrupts odorant-evoked neurotransmitter release from the olfactory nerve

Fourteen OMP-spH mice were randomly assigned to receive unilateral intranasal infusions of one of three different concentrations of $MnCl_2$ (200 μg, n = 4; 20 μg, n = 6; 2 μg, n = 4) and a contralateral infusion of vehicle solution. Two days after infusion, mice were anesthetized and odorant-evoked synaptic input to olfactory bulb glomeruli was imaged through a cranial window.

As shown in Fig. 1A, after a 200 μg infusion of $MnCl_2$ odorant-evoked neurotransmitter release from the olfactory nerve was greatly reduced. The number of glomeruli receiving measurable synaptic input on the Mn-exposed side was significantly reduced to 9 ± 6% of the glomeruli receiving input on the contralateral control side (one-sample t-test, hypothesized mean 100% of control; $p < 0.001$). As shown in Fig. 1A (right panel), the responses that were observed were significantly shifted towards smaller amplitudes than control responses (Kolmogorov-Smirnov test, $z = 5.36$, $p < 0.001$; Mann-Whitney U-test, $z = 10.87$, $p < 0.001$).

These effects on the number of glomeruli receiving input were significantly dose dependent (one-way ANOVA, $F_{2,11} = 12.06$, $p = 0.002$), as shown in Fig. 1D. A tenfold lower dose of Mn (20 μg $MnCl_2$, Fig. 1B) produced a smaller but still significant reduction in response amplitudes (K-S test, $z = 3.01$, $p < 0.001$; U-test, $z = 4.65$, $p < 0.001$) and a small reduction in the number of glomeruli receiving input (67 ± 13% of control; one-sample t-test, $p = 0.055$). A hundredfold lower intranasal dose (2 μg $MnCl_2$, Fig. 1C) caused a modest but still significant reduction in response amplitudes (K-S test, $z = 1.948$, $p = 0.001$; U-test, $z = 3.96$, $p < 0.001$), and no significant change in the number of glomeruli receiving measurable synaptic input (91 ± 6% of control; one-sample t-test, $p = 0.24$).

3.2 Manganese reduces nerve-shock evoked transmitter release from the olfactory nerve

The observed deficits in odorant-evoked exocytosis after Mn-exposure could result from either a peripheral effect on the olfactory epithelium (e.g. inflammation or disruption of olfactory transduction) or from a central effect occurring in the olfactory nerve layer of the olfactory bulb. To dissociate these possibilities, we used ten OMP-spH mice to visualize exocytosis evoked by electrical stimulation of the bulb's olfactory nerve layer *in vivo* in Mn- and vehicle-exposed olfactory bulbs. Two days after 200 μg $MnCl_2$ or vehicle infusion, the bone and dura overlying the dorsal olfactory bulbs were removed and a concentric bipolar stimulating electrode was positioned onto fluorescent ORN axon bundles under visual guidance by an experimenter blind to the experimental condition of the mouse. A total of 74 stimulation locations were tested in eleven olfactory bulbs from ten mice, evenly distributed (37 each) between Mn-exposed and vehicle-exposed bulbs. As shown in Fig. 2, electrical stimulation evoked measurable spH signals in only 31% as many glomeruli in Mn-exposed olfactory bulbs as in vehicle-exposed bulbs (Chi-square test $\chi^2 = 32.67$, $p < 0.001$). The modest number of spH signals that were observed in Mn-exposed bulbs were not significantly different in amplitude than those in vehicle-exposed bulbs (K-S test, $z = 0.97$, $p = 0.301$, Fig. 2D). These results demonstrate that the effects of Mn were not confined to the olfactory epithelium but directly affect presynaptic function in the brain's olfactory bulb.

3.3 The reduction in stimulus-evoked neurotransmitter release is not accompanied by histopathology

To evaluate whether the observed reduction in neurotransmitter release from presynaptic terminals was accompanied by histopathological changes in the olfactory nerve projection to the olfactory bulb, we perfused all mice from the highest dose exposure group (200 μg) after imaging along with four additional animals not included in the analysis of olfactory nerve physiology (total n = 8) and sectioned their olfactory bulbs for histological analysis. ORN axons and synaptic terminals were visualized by GFP fluorescence in neutralized histological sections, yielding clear images of the olfactory nerve innervation of individual olfactory bulb glomeruli (Fig. 3A–D, green fluorescence). DAPI nuclear stain visualized rings of periglomerular interneurons (Fig. 3A–D, blue fluorescence). Unsurprisingly, we did not observe any changes in the number or gross structure of olfactory bulb glomeruli or periglomerular rings. Importantly, the optical density of spH fluorescence was not significantly different between Mn-exposed and vehicle-exposed bulbs in the same sections (mean 88 ± 6% of control, one-group t-test, $p = 0.09$). This indicates that the density of ORN axonal projections remained intact after Mn exposure in the same animals that exhibited a > 90% reduction in neurotransmitter release.

Olfactory bulb glomeruli are surrounded by a shell of juxtaglomerular interneurons that express a variety of neurotransmitters and calcium binding proteins (Parrish-Aungst et al., 2007; Kosaka and Kosaka 2011) and have the capacity to presynaptically modulate neurotransmitter release from the olfactory nerve via dopamine and GABA (Ennis et al., 2001; McGann et al., 2005). Two of these molecularly-defined subpopulations have been reported to exhibit adaptive neurochemical plasticity in response to prolonged reductions in sensory input (Philpot et al., 1997, Baker et al., 1988). Expression of tyrosine hydroxlase (TH, the rate-limiting enzyme in dopamine synthesis) is greatly downregulated in TH-positive periglomerular neurons by manipulations that reduce activity in ORNs, including naris occlusion (Baker et al. 1988) and exposure to methyl bromide gas (Weruaga et al. 2000). The intracellular calcium binding protein calbindin-d28k (CBD) is expressed in a different subset of periglomerular interneurons and has also been shown to be downregulated when ORN activity is reduced by sensory deprivation (Philpot et al. 1997). To confirm empirically that the reductions in neurotransmitter release reported here are not a consequence of adaptive changes in these interneurons, we used fluorescent

immunohistochemical labeling to visualize TH and CBD expression. In four mice exposed to 200 μg $MnCl_2$, the optical density of TH- and CBD-associated immunofluorescence was measured in the glomerular layer of Mn-exposed and vehicle-exposed olfactory bulbs. The ratio of immunofluorescence on the Mn-exposed side to that on the vehicle exposed side was computed for each animal, providing a within-subjects design. For TH labeling (Fig. 3A & B, red fluorescence), Mn-exposed bulbs exhibited the same juxtaglomerular immunofluorescence as vehicle control (mean 97 ± 6% of control; one-sample t-test, $p = 0.63$). For CBD labeling (Fig. 3C & D, red fluorescence), immunofluorescence in olfactory bulbs on the Mn-exposed side was also not different from that in bulbs on the vehicle-exposed side (mean 96 ± 3% of control, one-sample t-test, $p = 0.28$). These proteins have both been reported to exhibit significant plasticity in response to olfactory nerve damage (Philpot et al., 1997, Baker et al., 1988) or senescence (Choi et al., 2010; Moyer et al., 2011), but changes in their expression patterns do not appear to contribute to the observed changes in olfactory nerve function. However, we cannot rule out the possibility that Mn-exposure alters the activity of TH independent of its expression (Lehmann et al., 2006).

4. Discussion

Here we use optical imaging and anatomical assays to investigate the pathophysiological effects of acute intranasal exposure to manganese. We find that a single intranasal instillation of 200 μg $MnCl_2$ almost completely eliminates odorant-evoked neurotransmitter release from the olfactory nerve, while 2 μg is sufficient to cause measurable pathophysiology using olfactory stimuli (Fig. 1). Importantly, direct electrical stimulation in the olfactory bulb's olfactory nerve layer also failed to evoke normal transmitter release, demonstrating that this effect is at least partially caused by a disruption of presynaptic function in the central nervous system (Fig. 2). No corresponding histopathological or neurochemical changes were observed, suggesting that at these doses the effects of Mn exposure are primarily physiological.

Because of the similarity between the extrapyramidal motor symptoms in manganism and in idiopathic Parkinsonism, studies of the mechanisms of manganese-induced pathophysiology have focused on the dopaminergic circuitry of the basal ganglia. However, evidence from human patients and non-human primate models indicates that unlike idiopathic Parkinson's disease, manganese-induced Parkinsonism does not include degeneration of dopaminergic neurons in the substantia nigra pars compacta (Yamada et al., 1986; reviewed in Perl and Olanow 2007), does not disrupt dopamine synthesis (Wolters et al., 1989; Shinotoh et al., 1997), and is not improved by L-DOPA therapy (Lu et al., 1994). Nonetheless, amphetamine challenge elicits less dopamine release (as inferred from its competition with radiolabeled raclopride) in the basal ganglia of a Mn-exposed non-human primate model, suggesting a potential presynaptic mechanism of action for Mn neurotoxicity in dopaminergic neurons (Guilarte et al., 2006; Guilarte et al., 2008b). The present findings use synaptopHluorin imaging and electrical stimulation to provide the first direct evidence that Mn can indeed disrupt neurotransmitter release from the presynaptic terminal after exposure. Importantly, the demonstration of these effects on glutamatergic ORNs indicate that Mn's effects are not confined to dopaminergic neurons or the basal ganglia, suggesting that the pleiotropic neurological consequences of Mn exposure may derive from a widespread influence on exocytosis wherever the element accumulates.

The most likely mechanism for Mn's actions is the disruption of presynaptic calcium signaling (Meiri and Rahaminoff 1972). Neurotransmitter release from ORN synaptic terminals exhibits a highly non-linear relationship between calcium concentration and exocytosis (Murphy et al., 2004; Wachowiak et al., 2005). Consequently, modest reductions in stimulus-evoked intracellular calcium fluxes can produce large decreases in

neurotransmitter release (Wachowiak et al., 2005). While Mn is an essential element, excessive accumulation of Mn could disrupt presynaptic calcium signaling in multiple ways. First, Mn ions can block the conotoxin-sensitive N-type calcium conductance (Castelli et al., 2003), which conducts the majority of the action potential-evoked calcium influx that occurs in ORN presynaptic terminals (Wachowiak et al., 2005). Interestingly, this is also the principal calcium conductance mediating dopamine release in the striatum (Mitchell and Adams 1993), so this shared mechanism could conceivably explain the reduction in neurotransmitter release observed there (Guilarte et al., 2008b). Mn could also disrupt intracellular calcium dynamics (as it does in astrocyte networks - see Tjalkens et al., 2006) by competing with divalent metal transporters that regulate calcium levels in the cytosol and intracellular stores, including mitochondria (see Verity 1999). Several calcium-independent mechanisms of action could also plausibly account for the reduction in stimulus evoked neurotransmitter release. Mn may disrupt the molecular machinery of exocytosis (Guilarte et al., 2008a; Uversky et al., 2001) or disrupt glial function including glutamate recycling (Erikson and Aschner 2002; Zwingmann et al., 2003). Finally, our data do not allow us to rule out a Mn-induced reduction in axonal excitability or conduction (which would have made it more difficult to elicit an action potential volley in Mn-exposed axons in our nerve shock experiments), though there is little evidence for this in the literature (Meiri and Rahaminoff 1972).

The concentrations used in this study were selected (based on preliminary data) to cover the full dynamic range of concentrations that produce differential effects, and in fact the effects ranged from significant but modest in size (at 2 μg $MnCl_2$) to near complete suppression of neurotransmitter release (200 μg). Many factors make it difficult to relate this dose range to human occupational exposures, including the differences in duration (acute vs chronic), delivery (liquid instillation vs. inhaled aerosol), nasal anatomy and tidal volume (mouse vs. human), and chemical form (chloride salt vs. oxides, phosphates, etc.). However, the average welder is chronically exposed to aerosolized Mn concentrations of about 250 μg / m^3 of air (Flynn and Susi 2010), and the OSHA Permissible Exposure Limit is 5000 $\mu g/m^3$ of air. It seems plausible that such exposures could indeed achieve olfactory Mn concentrations comparable to those induced here. Other routes of Mn exposure, such as systemic injection during drug abuse (Stepens et al., 2008; Sikk et al., 2010) and hepatic failure (Hauser et al., 1994), can also cause Mn accumulation in the olfactory bulb and could potentially achieve comparable regional concentrations.

The literature on the olfactory sensory consequences of Mn exposure is sparse. Significant olfactory dysfunction was reported in welders in the Bay Bridge Welder Study compared to matched controls, but the degree of olfactory impairment was not clearly related to blood Mn concentration (Bowler et al., 2007; Antunes et al., 2007). Perhaps because it is uniquely vulnerable to external toxicants, the olfactory system is highly plastic. This allows sensory learning to compensate for even severe toxicant-induced pathophysiology in the olfactory nerve (Czarnecki et al., 2012). Physiological techniques such as magnetic resonance imaging (Zald and Pardo 2000) or measurement of olfactory event-related potentials (Lötsch and Hummel, 2006; Scott and Scott-Johnson 2002) might thus reveal Mn-induced neurological deficits that are masked in conventional behavioral assays.

We found that while electrical stimulation evoked neurotransmitter release in many fewer glomeruli in Mn-exposed bulbs than in control bulbs, the responses that did occur in Mn-exposed bulbs were unexpectedly similar in size to controls. Because each individual glomerulus receives axonal projections from a corresponding sub-population of ORNs that all express the same odorant receptor (see Wilson and Mainen 2006 for a review), this result suggests that some ORN subpopulations were strongly affected by Mn while others showed little effect. It is possible that in addition to expressing different odorant receptors these

populations also differentially express some other factor that confers a selective vulnerability to Mn, or alternatively that differential stimulation of ORN sub-populations by the olfactory environment causes corresponding differences in the uptake of Mn (e.g. via activation of Mn-fluxing cyclic nucleotide-gated cation channels, see Piggott et al. 2006).

In addition to inducing a similar set of extrapyramidal motor symptoms to idiopathic Parkinson's disease, Mn-exposure has been reported to accelerate the development of PD (Racette et al., 2005). The incidence of PD is also more than 75% higher in geographic regions that include high industrial release of Mn than in control regions (Willis et al., 2010). Mn-exposure results in elevated Mn concentrations (Bonilla et al., 1994) and impaired neurotransmitter release in both the olfactory bulb (Figs. 2 and 3) and the basal ganglia (Guilarte et al., 2008b). These may correspond to the olfactory deficits and extrapyramidal motor symptoms typical of PD (Haehner et al., 2009; Guilarte et al., 2010a). Preclinical impairments in neurotransmitter release induced by Mn exposure could potentially render these regions more vulnerable to subsequent degeneration, such as the loss of dopaminergic input to the striatum in PD (Burch and Sheerin 2005).

Acknowledgments

This work was supported by grant R00 DC009442 from the National Institute on Deafness and Other Communication Disorders to JPM, grants P30 ES005022 and T-32 ES07148 from the National Institute of Environmental Health Sciences, and a grant from the Busch Biomedical Research fund to JPM.

References

Antunes MB, Bowler R, Doty RL. San Francisco/Oakland Bay Bridge welder study: olfactory function. Neurology. 2007; 69:1278–84. [PubMed: 17875916]

Aschner M, Erikson KM, Hernández EH, Tjalkens R. Manganese and its role in Parkinson's disease: From transport to neuropathology. Neuromolecular Med. 2009; 11:252–66. [PubMed: 19657747]

Avila DS, Colle D, Gubert P, Palma AS, Puntel G, Manarin F, Noremberg S, Nascimento PC, Aschner M, Rocha JB, Soares FA. A possible neuroprotective action of a vinyl telluraide against Mn-induced neurotoxicity. Toxicol Sci. 2010; 115:194–201. [PubMed: 20133376]

Baker H, Towle AC, Margolis FL. Differential afferent regulation of dopaminergic and GABAergic neurons in the mouse main olfactory bulb. Brain Res. 1988; 450:69–80. [PubMed: 2900047]

Barbeau A, Inoué N, Cloutier T. Role of manganese in dystonia. Adv Neurol. 1976:339–52. [PubMed: 821321]

Barhoumi R, Faske J, Liu X, Tjalkens RB. Manganese potentiates lipopolysaccharide-induced expression of NOS2 in C6 glioma cells through mitochrondrial-dependent activation of nuclear factor kappaB. Brain Res Mol Brain Res. 2004; 122:167–79. [PubMed: 15010209]

Bonilla E, Salazar E, Villasmil JJ, Villalobos R. The regional distribution of manganese in the normal human brain. Neurochem Res. 1982; 7:221–7. [PubMed: 7121709]

Bonilla E, Arrieta A, Castro F, Dávila JO, Quiroz I. Manganese toxicity: free amino acids in the striatum and olfactory bulb of the mouse. Invest Clin. 1994; 35:175–81. [PubMed: 7734520]

Bouchard M, Mergler D, Baldwin M, Panisser M, Bowler R, Roels HA. Neurobehavioral functioning after cessation of manganese exposure: a follow-up after 14 years. Am J Ind Med. 2007; 50:831–40. [PubMed: 17096374]

Bowler RM, Mergler D, Sassine MP, Larribe F, Hudnell K. Neuropsychiatric effects of manganese on mood. Neurotoxicology. 1999; 20:367–78. [PubMed: 10385897]

Bowler RM, Roels HA, Nakagawa S, Drezgic M, Diamond E, Park R, Koller W, Bowler RP, Mergler D, Bouchard M, Smith D, Gwiazda R, Doty RL. Dose-effect relationships between manganese exposure and neurological, neuropsychological, and pulmonary function in confined space bridge welders. Occup Environ Med. 2007; 64:167–77. [PubMed: 17018581]

Bozza T, McGann JP, Mombaerts P, Wachowiak M. In vivo imaging of neuronal activity by targeted expression of a genetically encoded probe in the mouse. Neuron. 2004; 42:9–21. [PubMed: 15066261]

Brenneman KA, Cattley RC, Ali SF, Dorman DC. Manganese-induced developmental neurotoxicity in the CD rat: is oxidative damage a mechanism of action? Neurotoxicology. 1999; 20:477–88. [PubMed: 10385906]

Brenneman KA, Wong BA, Buccllato MA, Costa ER, Gross EA, Dorman DC. Direct olfactory transport of inhaled manganese ((54)MnCl(2)) to the rat brain: toxicokinetic investigations in a unilateral nasal occlusion model. Toxicol Appl Pharmacol. 2000; 169:238–48. [PubMed: 11133346]

Brouillet EP, Shinobu L, McGarvey U, Hochberg F, Beal MF. Manganese injection into the rat striatum produces excitotoxic lesions by impairing energy metabolism. Exp Neurol. 1993; 120:89–94. [PubMed: 8477830]

Buck L, Axel R. A novel mulitgene family may encode odorant receptors: a molecular basis for odor recognition. Cell. 1991; 65:175–87. [PubMed: 1840504]

Burch D, Sheerin F. Parkinson's Disease. Lancet. 2005; 365:622–7. [PubMed: 15708109]

Castelli L, Tanzi F, Taglietti V, Magistretti J. Cu2+, Co2+, and Mn2+ modify the gating kinetics of high-voltage-activated Ca2+ channels in rat paleocortical neurons. J Membr Biol. 2003; 195:121–36. [PubMed: 14724759]

Cerosimo MG, Koller WC. The diagnosis of manganese-induced parkinsonism. Neurotoxicology. 2006; 27:340–6. [PubMed: 16325915]

Chandra S, Gallardo G, Fernanadez-Chacon R, Schluter OM, Sudhof TC. Alpha-synuclein cooperates with CSPalpha in preventing neurodegeneration. Cell. 2005; 123:383–96. [PubMed: 16269331]

Cheh MA, Millonig JH, Roselli LM, Ming X, Jacobsen E, Kamdar S, Wagner GC. En2 knockout mice display neurobehavioral and neurochemical alterations relevant to autism spectrum disorder. Brain Res. 2006; 1116:166–76. [PubMed: 16935268]

Choi JH, Lee CH, Yoo KY, Hwang IK, Lee IS, Lee YL, Shin HC, Won MH. Age-related change in calbindin-D28k, parvalbumin, and calretinin immunoreactivity in the dog main olfactory bulb. Cell Mol Neurobiol. 2010; 30:1–12. [PubMed: 19533334]

Cotman CW, Foster A, Lanthorn T. An overview of glutamate as a neurotransmitter. Adv Biochem Psychopharmacol. 1981; 27:1–27. [PubMed: 6108689]

Couper J. On the effects of black oxide of manganese when inhaled into the lungs. British Annals of Medicine, Pharmacy, Vital Statistics and General Science. 1873; 1:41–2.

Czarnecki LA, Moberly AH, Rubinstein T, Turkel DJ, Pottackal J, McGann JP. In vivo visualization of olfactory pathophysiology induced by intranasal cadmium exposure in mice. Neurotoxicology. 2011; 32:441–9. [PubMed: 21443902]

Czarnecki LA, Moberly AH, Turkel DJ, Rubinstein T, Pottackal J, Rosenthal MC, McCandlish EFK, Buckley B, McGann JP. Functional rehabilitation of cadmium-induced neurotoxicology despite persistent peripheral pathophysiology in the olfactory system. J Toxicol Sci. 2012; 126:534–44.

Desole MS, Esposito G, Migheli R, Fresu L, Sircana S, Miele M, De Natale G, Miele E. Allopurinol protects against manganese-induced oxidative stress in the striatum and in the brainstem of the rat. Neurosci Lett. 1995; 192:73–6. [PubMed: 7675324]

Donaldson J, Cloutier T, Minnich JL, Barbeau A. Trace metals and biogenic amines in rat brain. Adv Neurol. 1974; 5:245–52. [PubMed: 4440574]

Dorman DC, Brenneman KA, McElveen AM, Lynch SE, Roberts KC, Wong BA. Olfactory transport : a direct route of delivery of inhaled manganese phosphate to the rat brain. J Toxicol Environ Health. 2002; 65:1493–511.

Dydak U, Jiang YM, Long LL, Zhu H, Chen J, Li WM, Edden RA, Hu S, Fu X, Long Z, Mo XA, Meier D, Harezlak J, Aschner M, Murdoch JB, Zheng W. In vivo measurement of brain GABA concentrations by magnetic resonance spectroscopy in smelters occupationally exposed to manganese. Environ Health Perspect. 2011; 119:219–24. [PubMed: 20876035]

Ennis M, Zhou FM, Ciombor KJ, Aroniadou-Anderjaska V, Hayar A, Borrelli E, Zimmer LA, Margolis F, Shipley MT. Dopamine D2 receptor-mediated presynaptic inhibition of olfactory nerve terminals. J Neurophysiol. 2001; 86:2986–97. [PubMed: 11731555]

Eriksson H, Magiste K, Plantin LO, Fonnum F, Hedstrom KG, Theodorsson-Norheim E, Kristensson K, Stålberg E, Heilbronn E. Effects of manganese oxide on monkeys as revealed by a combined neurochemical, histological, and neurophysiological evaluation. Arch Toxicol. 1987; 61:46–52. [PubMed: 3439874]

Erikson K, Aschner M. Manganese causes differential regulation of glutamate transporter (GLAST) taurine transporter and metallothionein in cultured rat astrocytes. Neurotoxicology. 2002; 23:595–602. [PubMed: 12428731]

Flynn MR, Susi P. Manganese, iron, and total particulate exposures to welders. J Occup Environ Hyg. 2010; 7:115–26. [PubMed: 20013450]

Gavin CE, Gunter KK, Gunter TE. Manganese and calcium transport in mitochondria: implications for manganese toxicity. Neurotoxicology. 1999; 20:445–53. [PubMed: 10385903]

Gianutsos G, Morrow GR, Morris JB. Accumulation of manganese in rat brain following intranasal administration. Fund Appl Toxicol. 1997; 37:102–5.

Guilarte T, Chen MK, McGlothan JL, Verina T, Wong DF, Zhou Y, Alexander M, Rohde CA, Syversen T, Decamp E, Koser AJ, Fritz S, Gonczi H, Anderson D, Schneider JS. Nigrostriatal dopamine system dysfunction and subtle motor deficits in manganese-exposed non-human primates. Exp Neurol. 2006; 202:381–90. [PubMed: 16925997]

Guilarte T. Manganese and Parkinson's disease: a critical review and new findings. Environ Health Perspect. 2010a; 118:1071–80. [PubMed: 20403794]

Guilarte T. APLP1, Alzheimer's-like pathology and neurodegeneration in the frontal cortex of manganese-exposed non-human primates. Neurotoxicology. 2010b; 31:572–4. [PubMed: 20188756]

Guilarte TR, Burton NC, Verina T, Prabhu BB, Becker KG, Syversen T, Schneider JS. Increased APLP1 expression and neurodegeneration in the frontal cortex of manganese-exposed non-human primates. J Neurochem. 2008a; 105:1948–59. [PubMed: 18284614]

Guilarte TR, Burton NC, McGlothan JL, Verina T, Zhou Y, Alexander M, Pham L, Griswold M, Wong DF, Syversen T, Schneider S. Impairment of nigrostriatal dopamine transmission by manganese is mediated by pre-synaptic mechanism(s): Implications to manganese-induced parkinsonism. J Neurochem. 2008b; 107:1236–47. [PubMed: 18808452]

Haehner A, Boesveldt S, Berendse HW, Mackay-Sim A, Fleischmann J, Silburn PA, Johnston A, Mellick GD, Herting B, Reichmann H, Hummel T. Prevalence of smell loss in Parkinson's disease-A multicenter study. Parkinsonism Relat Disord. 2009; 15:490–4. [PubMed: 19138875]

Hauser RA, Zesiewicz TA, Rosemurgy AS, Martinez C, Olanow CW. Manganese intoxication and chronic liver failure. J Neurol. 1994; 250:1335–9.

Hazell AS, Norenberg MD. Manganese decreases glutamate uptake in cultured astrocytes. Neurochem Res. 1997; 22:1443–7. [PubMed: 9357008]

Henriksson J, Tjälve H. Manganese taken up into the CNS via the olfactory pathway in rats affects astrocytes. Toxicol Sci. 2000; 55:392–8. [PubMed: 10828272]

Hussain S, Lipe GW, Slikker W, Ali SF. The effects of chronic exposure of manganese on antioxidant enzymes in different regions of rat brain. Neurosci Res Commun. 1997; 21:135–44.

Iregren A. Using psychological tests for the early detection of neurotoxic effects of low level manganese exposure. Neurotoxicology. 1994; 15:671–7. [PubMed: 7854605]

Kosaka T, Kosaka K. "Interneurons" in the olfactory bulb revisited. Neurosci Res. 2011; 69:93–9. [PubMed: 20955739]

Laohaudomchok W, Lin X, Herrick RF, Fang SC, Cavallari JM, Shrairman R, Landau A, Christiani DC, Weisskopf MG. Neuropsychological effects of low-level manganese exposure in welders. Neurotoxicology. 2011; 32:171–179. [PubMed: 21192973]

Lehmann IT, Bobrovskaya L, Gordon SL, Dunkley PR, Dickson PW. Differential regulation of the human tyrosine hydroxylase isoforms via hierarchical phosphorylation. J Biol Chem. 2006; 281:17644–17651. [PubMed: 16644734]

Liu X, Sullivan KA, Madl JE, Legare M, Tjalkens RB. Manganese-induced neurotoxicity: the role of astroglial-derived nitric oxide in striatal interneuron degeneration. Toxicol Sci. 2006; 91:521–31. [PubMed: 16551646]

Lötsch J, Hummel T. The clinical significance of electrophysiological measures of olfactory function. Behav Brain Res. 2006; 170:78–83. [PubMed: 16563529]

Lu CS, Huang CC, Chu NS, Calne DB. Levodopa failure in chronic manganism. Neurology. 1994; 44:1600–2. [PubMed: 7936281]

McGann JP, Pirez N, Gainey MA, Muratore C, Elias AS, Wachowiak M. Odorant representations are modulated by feedback but not lateral presynaptic inhibition of olfactory sensory neurons. Neuron. 2005; 48:1039–1053. [PubMed: 16364906]

Meiri U, Rahamimoff R. Neuromuscular transmission: inhibition by manganese ions. Science. 1972; 176:308–9. [PubMed: 5019787]

Mergler D, Baldwin M, Bélanger S, Larribe F, Beuter A, Bowler R, Panisset M, Edwards R, de Geoffroy A, Sassine MP, Hudnell K. Manganese neurotoxicity, a continuum of dysfunction: results from a community based study. Neurotoxicology. 1999; 20:327–42. [PubMed: 10385894]

Miesenböck G, De Angelis DA, Rothman JE. Visualizing secretion and synaptic transmission with pH-sensitive green fluorescent proteins. Nature. 1998; 394:192–5. [PubMed: 9671304]

Milatovic D, Gupta RC, Yu U, Zaia-Milatovic S, Aschner M. Protective effects of antioxidants and anti-inflammatory agents against manganese-induced oxidative damage and neuronal injury. Toxicol Appl Pharmacol. 2011; 256:219–26. [PubMed: 21684300]

Mitchell K, Adams RN. Comparison of the effects of voltage-sensitive calcium channel antagonism on the electrically stimulated release of dopamine and norepinephrine in vivo. Brain Res. 1993; 604:349–53. [PubMed: 8457864]

Mombaerts P, Wang F, Dulac C, Chao SK, Nemes A, Mendelsohn M, Edmondson J, Axel R. Visualizing an olfactory sensory map. Cell. 1996; 87:675–8. [PubMed: 8929536]

Moyer JR Jr, Furtak SC, McGann JP, Brown TH. Aging-related changes in calcium-binding proteins in rat perirhinal cortex. Neurobiol Aging. 2011; 32:1693–706. [PubMed: 19892435]

Murphy GL, Glickfeld LL, Balsen Z, Isaacson JS. Sensory neuron signaling to the brain: properties of transmitter release from olfactory nerve terminals. J Neurosci. 2004; 24:3023–30. [PubMed: 15044541]

Pal PK, Samil A, Caine DB. Manganese neurotoxicity: a review of clinical features, imaging and pathology. Neurotoxicology. 1999; 20:227–38. [PubMed: 10385886]

Parrish-Aungst S, Shipley MT, Erdelyi F, Szabo G, Puche AC. Quantitative analysis of neuronal diversity in the mouse olfactory bulb. J Comp Neurol. 2007; 501:825–36. [PubMed: 17311323]

Pentschew A, Ebner FF, Kovatch RM. Experimental manganese encephalopathy in monkeys. A preliminary report. J Neuropathol Exp Neurol. 1963; 22:488–99. [PubMed: 14045007]

Perl DP, Olanow CW. The neuropathology of manganese-induced Parkinsonism. J Neuropathol Exp Neurol. 2007; 66:675–82. [PubMed: 17882011]

Philpot BD, Lim JH, Brunjes PC. Activity-dependent regulation of calcium-binding proteins in the developing rat olfactory bulb. J Comp Neurol. 1997; 387:12–26. [PubMed: 9331168]

Piggott LA, Hassell KA, Berkova Z, Morris AP, Silberbach M, Rich TC. Natriuretic peptides and nitric oxide stimulate cGMP synthesis in different cellular compartments. J Gen Physiol. 2006; 128:3–14. [PubMed: 16769793]

Pírez N, Wachowiak M. In vivo modulation of sensory input to the olfactory bulb by tonic and activity-dependent presynaptic inhibition of receptor neurons. J Neurosci. 2008; 28:6360–71. [PubMed: 18562606]

Racette BA, Tabbal SD, Jennings D, Good L, Perlmutter JS, Evanoff B. Prevalence of parkinsonism and relationship to exposure in a large sample of Alabama welders. Neurology. 2005; 64:230–5. [PubMed: 15668418]

Roels H, Sarhan MJ, Hanotiau I, de Fays M, Genet P, Bernard A, Buchet JP, Lauwerys R. Preclinical toxic effects of manganese in workers from a Mn salts and oxides producing plant. Sci Total Environment. 1985; 42:201–6.

Roels HA, Ghyselen P, Buchet JP, Ceulemans E, Lauwerys RR. Assessments of the permissible exposure level to manganese in workers exposed to manganese dioxide dust. Br J Ind Med. 1992; 49:25–34. [PubMed: 1733453]

Schneider JS, Decamp E, Clark K, Bouquio C, Syversen T, Guilarte T. Effects of chronic manganese exposure on working memory in non-human primates. Brain Res. 2009; 1258:86–95. [PubMed: 19133246]

Scott JW, Scott-Johnson SE. The electroolfactogram: a review of its history and uses. Microsc Res Tech. 2002; 58:152–60. [PubMed: 12203693]

Shinotoh H, Snow BJ, Chu NS, Huange CC, Lu CS, Lee C, Takahashi H, Calne DB. Presynaptic and postsynaptic striatal dopaminergic function in patients with manganese intoxication: a positron emission tomography study. Neurology. 1997; 48:1053–6. [PubMed: 9109899]

Sikk K, Taba P, Haldre S, Bergquist J, Nyholm D, Askmark H, Danfors T, Sörensen J, Thurfjell L, Raininko R, Eriksson R, Flink R, Färnstrand C, Aquilonius SM. Clinical, neuroimaging and neurophysiological features in addicts with manganese-ephedrone syndrome. Acta Neurol Scand. 2010; 121:237–43. [PubMed: 20028341]

Soucy ER, Albeanu DF, Fantana AL, Murthy VN, Meister M. Precision and diversity in an odor map on the olfactory bulb. Nat Neurosci. 2009; 12:210–20. [PubMed: 19151709]

Spranger M, Schwab S, Desiderato S, Bonmann E, Krieger D, Fandrey J. Manganese augments nitric oxide synthesis in murine astrocytes: a new pathogenetic mechanism in manganism? Exp Neurol. 1998; 149:277–83. [PubMed: 9454637]

Stepens A, Logina I, Liguts V, Aldins P, Eksteina I, Platkajis A, Martinsone I, Terauds E, Rozentale B, Donaghy M. A Parkinsonian syndrome in methcathinone users and the role of manganese. N Engl J Med. 2008; 358:1009–17. [PubMed: 18322282]

Sunderman FW. Nasal toxicity, carcinogenicity, and olfactory uptake of metals. Ann Clin Lab Sci. 2001; 31:3–24. [PubMed: 11314863]

Takeda A, Sotogaku N, Oku N. Manganese influences the levels of neurotransmitters in synapses in rat brain. Neuroscience. 2002; 114:669–74. [PubMed: 12220568]

Taylor MD, Erikson KM, Dobson AW, Fitsanakis VA, Dorman DC, Aschner M. Effects of inhaled manganese on biomarkers of oxidative stress in the rat brain. Neurotoxicology. 2006; 27:788–97. [PubMed: 16842851]

Thompson K, Molina RM, Donaghey T, Schwob JE, Brain JD, Wessling-Resnick M. Olfactory uptake of manganese requires DMTI and is enhanced by anemia. Faseb J. 2007:223–30. [PubMed: 17116743]

Thompson KJ, Molina RM, Donaghey T, Savaliya S, Schwob JE, Brain JD. Manganese uptake and distribution in the brain after methyl bromide-induced lesions in the olfactory epithelia. Toxicol Sci. 2011; 120:163–72. [PubMed: 21177252]

Tjalkens RB, Zoran MJ, Mohl B, Barhoumi R. Manganese suppresses ATP-dependent intercellular calcium waves in astrocyte networks through alteration of mitochontrial and endoplasmic reticulum calcium dynamics. Brain Res. 2006; 1113:210–9. [PubMed: 16934782]

Tjälve H, Mejàre C, Borg-Neczak K. Uptake and transport of manganese in primary and secondary olfactory neurons in pike. Pharmacol Toxicol. 1995; 77:23–31. [PubMed: 8532608]

Tjälve H, Henriksson J, Talkvist J, Larsson BS, Lindquist NG. Uptake of manganese and cadmium from the nasal mucosa into the central nervous system via olfactory pathways in rats. Pharmacol Toxicol. 1996; 79:347–56. [PubMed: 9000264]

Uversky VN, Li J, Fink AL. Metal-triggered structural transformations, aggregation, and fibrillation of human alpha-synuclein. J Biol Chem. 2001; 276:44284–96. [PubMed: 11553618]

Verity MA. Manganese neurotoxicity: A mechanistic hypothesis. Neurotoxicology. 1999; 20:489–97. [PubMed: 10385907]

Vitarella D, Wong BA, Moss OR, Dorman DC. Pharmacokinetics of inhaled manganese phosphate in male Sprague-Dawley rats following subacute (14-day) exposure. Toxicol Appl Pharmacol. 2000; 163:279–85. [PubMed: 10702367]

Wachowiak M, McGann JP, Heyward PM, Shao Z, Puche AC, Shipley MT. Inhibition of olfactory receptor neuron input to olfactory bulb glomeruli mediated by suppression of presynaptic calcium influx. J Neurophysiol. 2005; 94:2700–12. [PubMed: 15917320]

Wedler FC, Ley BW, Grippo AA. Manganese(II) dynamics and distribution in glial cells cultured from chick cerebral cortex. Neurochem Res. 1989; 14:1129–35. [PubMed: 2480533]

Weruaga E, Briñón JG, Porteros A, Arévalo, Aijón J, Alonso JR. Expression of neuronal nitric oxide synthase/NADPH-diaphorase during olfactory deafferentation and regeneration. Eur J Neurosci. 2000; 12:1177–1193. [PubMed: 10762349]

Willis AW, Evanoff BA, Lian M, Galarza A, Wegrzyn MS, Racette BA. Metal emissions and urban incident parkinson's disease: a community health study of medicare beneficiaries by using geographic information systems. Am J Epidemiol. 2010; 172:1357–63. [PubMed: 20959505]

Wilson RI, Mainen ZF. Early events in olfactory processing. Annu Rev Neurosci. 2006; 29:163–201. [PubMed: 16776583]

Wolters EC, Huang CC, Clark C, Peppard RF, Okada J, Chu NS, Adam MJ, Ruth TJ, Li D, Calne DB. Positron emission tomography in manganese intoxication. Ann Neurol. 1989; 26:647–51. [PubMed: 2510588]

Yamada M, Ohno S, Okayasu I, Okeda R, Hatakeyama S, Watanabe H, Ushio K, Tsukagoshi H. Chronic Manganese poisoning: a neuropathological study with determination of manganese distribution in the brain. Acta Neuropathol. 1986; 70:273–8. [PubMed: 3766127]

Zald DH, Pardo JV. Functional neuroimaging of the olfactory system in humans. Int J Psychophysiol. 2000; 36:165–81. [PubMed: 10742571]

Zhang P, Wong TA, Lokuta KM, Turner DE, Vujisic K, Liu B. Microglia enhance manganese chloride-induced dopaminergic neurodegeneration: role of free radical generation. Exp Neurol. 2009; 217:219–30. [PubMed: 19268665]

Zwingmann C, Leibfritz D, Hazell AS. Energy metabolism in astrocytes and neurons treated with manganese: relation among cell-specific energy failure, glucose metabolism, and intercellular trafficking using multinuclear NMR-spectroscopic analysis. J Cereb Blood Flow Metab. 2003; 23:756–71. [PubMed: 12796724]

Highlights

- Acute Mn exposure dose-dependently disrupts odorant-evoked neurotransmitter release from ORNs.
- Direct ORN stimulation revealed pathophysiology occurs downstream of peripheral transduction.
- We found no evidence of histopathology even at Mn doses that suppressed neurotransmission by > 90%.

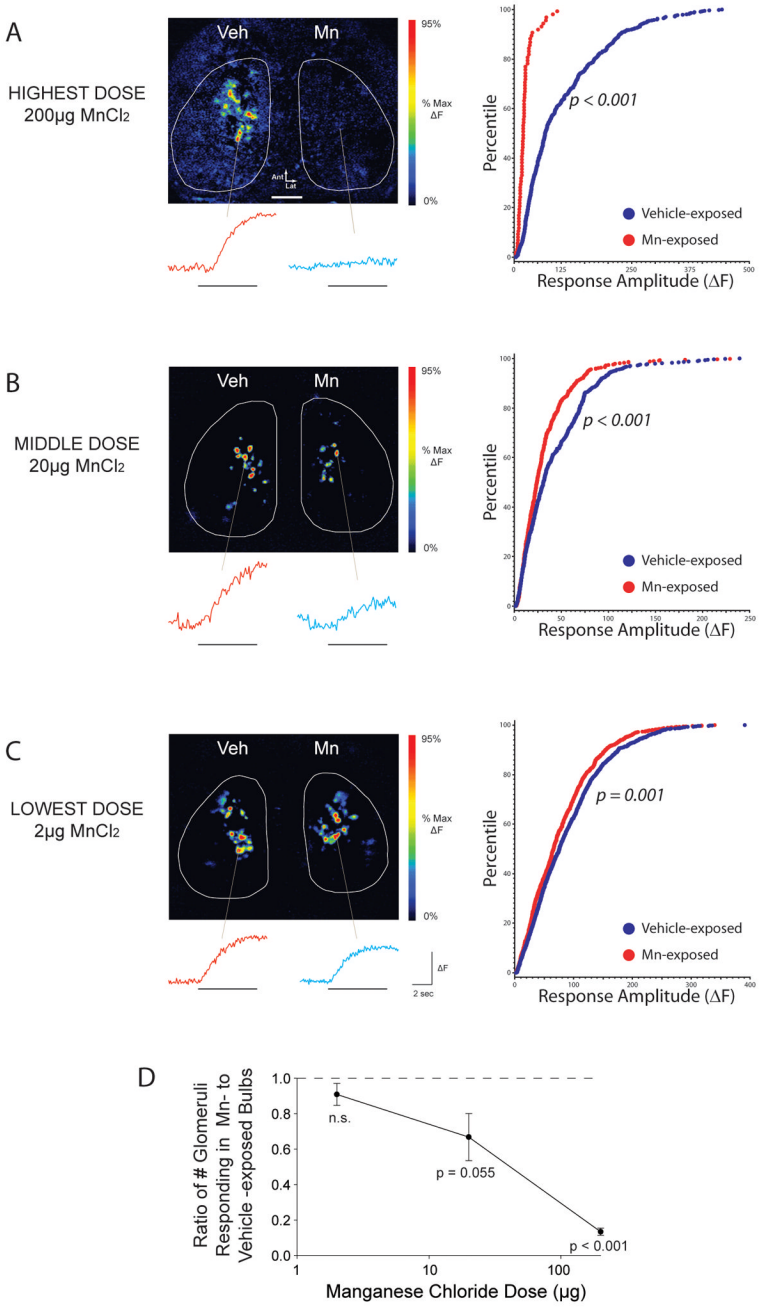

Figure 1. Intranasal instillation of manganese chloride dose-dependently reduces odorant-evoked neurotransmitter release from the olfactory nerve

(A–C Left) Odorant-evoked neurotransmitter release is visualized *in vivo* through a cranial window. Pseudocolored response maps show representative odorant-evoked increases in fluorescence relative to pre-odorant baseline across manganese doses. Individual traces display the change in fluorescence of the corresponding glomerulus during odorant presentation (denoted by the horizontal line). The odorant presented was 2-methyl-2-butenal in all three examples. The scale bar in A denotes 500 µm. (A–C Right) Cumulative distribution of glomerular response amplitudes in vehicle- and manganese- exposed olfactory bulbs. (D) Mn dose-dependently reduces the number of olfactory bulb glomeruli receiving odorant-evoked synaptic input, expressed as the ratio of the number of glomeruli

receiving input on the Mn-exposed side to that on the contralateral, vehicle-exposed side within each mouse tested. The dashed line at 1 represents no difference between Mn-exposed and vehicle-exposed olfactory bulbs.

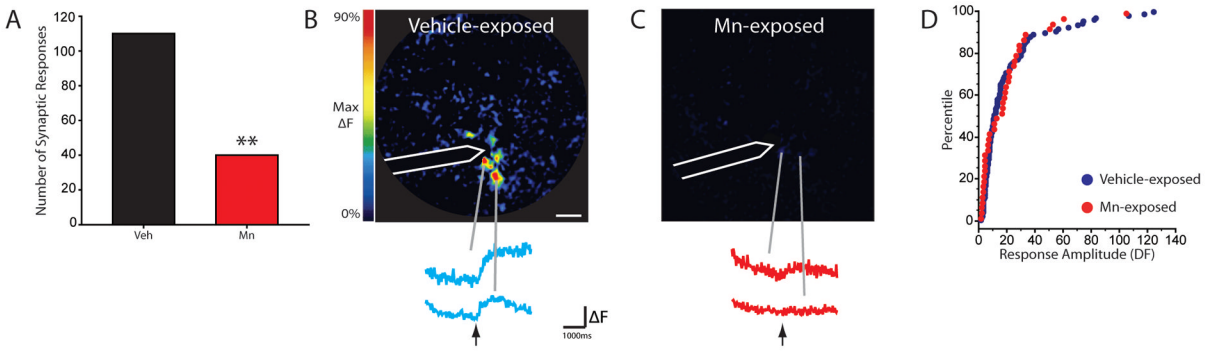

Figure 2. Intranasal instillations of manganese chloride reduce the number of nerve-shock evoked synaptic responses

(A) Plot showing the number of nerve-shock evoked glomerular responses is reduced on the manganese-exposed side compared to the vehicle-exposed side. (B–C) Pseudocolored response maps and showing single nerve-shock evoked spH signals scaled to the maximum of the response in C. Call outs show individual traces of fluorescence change in corresponding glomerulus before and after stimulation, as indicated by arrow. The white outline indicates electrode location. ** indicates $p < 0.001$. The white scale bar denotes 200 μm. (D) Cumulative distribution of nerve shock evoked glomerular response amplitudes in vehicle- and manganese-exposed bulbs.

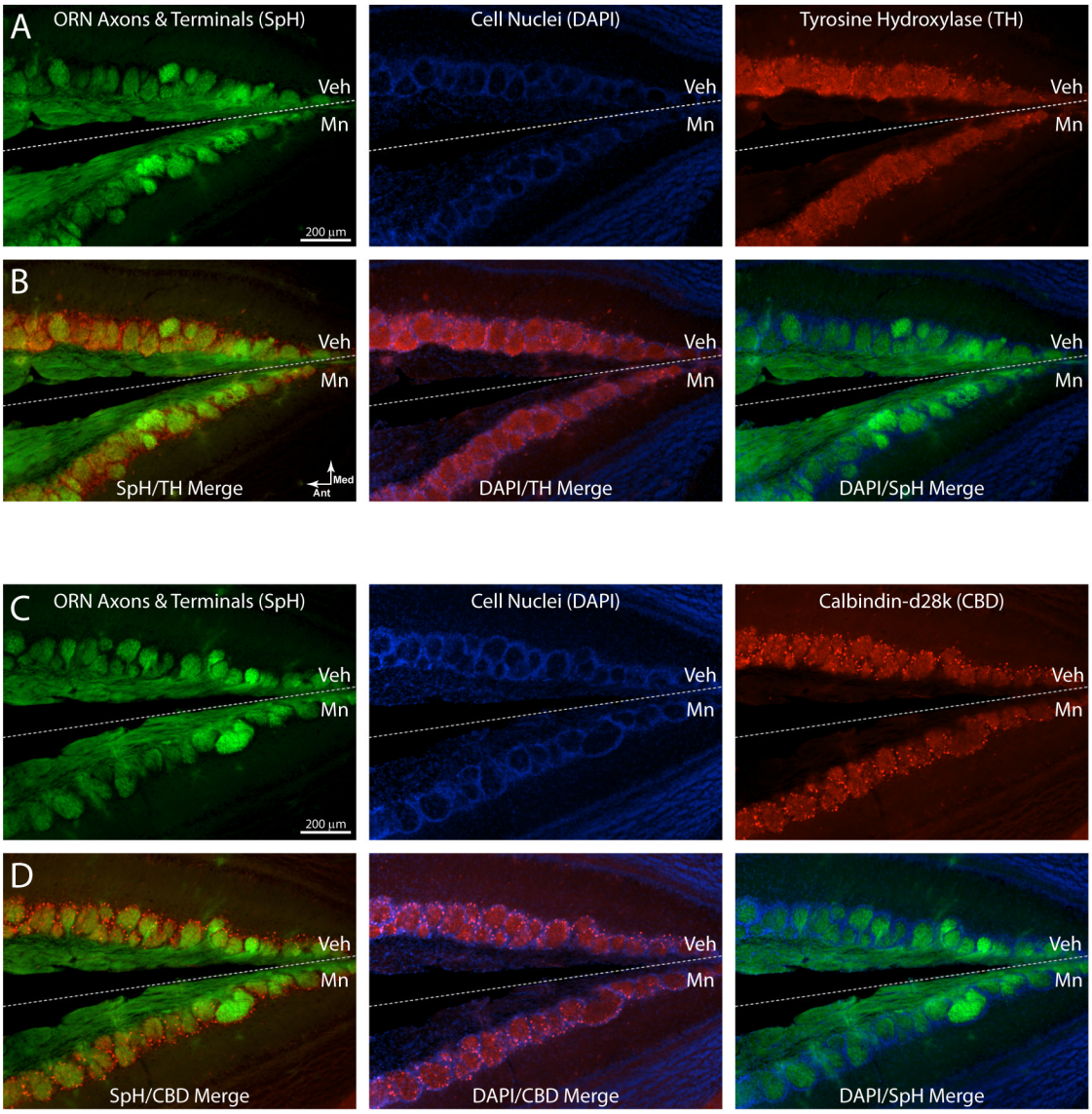

Figure 3. Morphological and immunohistochemical comparison of Mn- and vehicle-exposed olfactory bulbs

Images from a horizontal section showing the posterior part of two olfactory bulbs where they become adjacent along the midline (represented by the dashed line). The upper bulb in each image is ipsilateral to the intranasal vehicle instillation (Veh), while the lower bulb is ipsilateral to the intranasal 200 µg $MnCl_2$ instillation (Mn). Anterior is to the left and the vertex of the "V" shape is the midline of the mouse in all images. Rows A and B are all images from the same section, in which the green indicates spH fluorescence from ORN axons, blue indicates cell nuclei labeled with the nucleic acid stain DAPI, and red indicates AlexaFluor568 fluorescence from immunolabeled tyrosine hydroxylase. Rows C and D are images from a different section from the same mouse using the same colors except that red indicates AlexaFluor568 fluorescence from immunolabeled calbdindin-d28k. Rows B and D display the three possible color merged images from rows A and C, respectively, for comparison. No differences were observed between Mn-exposed and vehicle-exposed bulbs using any of these indicators. Note that while these images show a limited field of view of

the medial edge of each bulb for display purposes, data quantification was performed across the entire bulb.